Superlubricity of dry nanocontacts

2008 J. Phys.: Condens. Matter 20 354004

(http://iopscience.iop.org/0953-8984/20/35/354004)

IOP PUBLISHING JOURNAL OF PHYSICS: CONDENSED MATTER

J. Phys.: Condens. Matter **20** (2008) 354004 (5pp) doi:10.1088/0953-8984/20/35/354004

Superlubricity of dry nanocontacts

Enrico Gnecco, Sabine Maier[1] and Ernst Meyer

Department of Physics and NCCR Nanoscale Science, University of Basel, Klingelbergstrasse 82, 4056 Basel, Switzerland

Received 1 February 2008, in final form 28 March 2008
Published 11 August 2008
Online at stacks.iop.org/JPhysCM/20/354004

Abstract

We discuss how various forms of dry superlubricity, recently observed on the nanoscale, have been interpreted by simple phenomenological models. In particular, we review the cases of static and dynamic single-contact lubricity, thermolubricity, and structural lubricity. All these phenomena have been studied by friction force microscopy and explained using the classical Prandtl–Tomlinson model and its extensions, including thermal activation, temporal and spatial variations of the surface energy corrugation, and multiple-contact effects.

1. Introduction

The development of miniaturized mechanical components reaches its limits when surface-to-volume ratios become so high that wear and adhesion drastically reduce the lifetime of devices. This is a common issue in micro-electromechanical systems (MEMS), the operation of which is seriously affected by tribological problems [1–3]. Unfortunately, the phenomenological knowledge about macroscopic friction cannot be simply scaled down to the nanoscale. On the macroscale, friction can be reduced by using liquid lubricant, but this is not possible in MEMS, where interstitial features can easily reach molecular scales and traditional lubricants tend to coalesce [4]. Thus, there is a strong need to understand the mechanical behavior of sliding dry contacts a few nanometers in size and to develop new strategies to reduce or at least control friction on them.

The atomic force microscope (AFM) [5], and its further development as the friction force microscope (FFM) [6], is a suitable instrument to study the behavior of a single nanoscale contact. A sharp tip is moved over a surface and the torsion of a thin cantilever which sustains the tip is used to quantify friction between tip and surface. The first and most important observation obtained with FFM is that sliding on the nanoscale usually consists in a series of abrupt jumps between different equilibrium positions of the tip across the surface. Even if such a *stick–slip* motion is also apparent on the macroscale, for instance in the sliding of a piece of rubber, its peculiar feature on the nanoscale is that on crystalline surfaces this process repeats itself periodically every lattice spacing. The first observation of atomic stick–slip by Mate *et al* was reported on graphite [6]. Meanwhile, atomic-scale stick–slip has been experimentally observed on a variety of materials including insulators [7–9], metals [10, 11] and semiconductors [12]. Stick–slip motion results in high energy dissipation and should be avoided in delicate devices such as MEMS. One has to find a way to transform stick–slip into continuous frictionless sliding. Hirano and Shinjo introduced the term *superlubricity* for that frictionless state of motion [13].

The term *superlubricity* was originally intended to describe the state of ultralow friction achieved when two crystalline solid surfaces with incommensurate contact slide over each other. It is reminiscent of *superconductivity* and *superfluidity*, which refer to the vanishing of electrical resistivity and viscosity observed when some conductors and fluids are cooled below well-defined critical temperatures. Even if significant decreases of surface friction at the onset of superconductivity have been observed in experiments based on the quartz microbalance technique [14, 15], superlubric transitions on well-defined nanocontacts have been revealed by FFM in different ways. For instance, a state of vanishing friction between a sharp tip and a flat surface is expected whenever the normal load does not exceed a few nanonewtons. Here the term 'vanishing' means that no energy is released in the stick–slip process, but other dissipative mechanisms can still be present in the contact region. The superlubric threshold, at which stick–slip disappears, depends on the stiffness of tip and surface, as well as on the strength of the interaction potential between them. A clear observation of this transition has been reported for a silicon tip sliding on an NaCl surface by variation of the load on the contact [16]. More recently, we have shown that the transition can also be reached in a 'dynamic' way, by electromechanically exciting the tip at well-defined frequencies [17]. In such a case, the threshold load can be increased almost up to the yield pressure of the brittlest material, which is quite promising for applications to MEMS.

[1] Present address: Materials Science Division, Lawrence Berkeley National Laboratory, 1 Cyclotron Road, Berkeley, CA 94720, USA.

Another superlubric mechanism on dry contacts consists of sliding at ultralow speed (*thermolubricity*), so that thermally activated slips of the tip have enough time to completely destroy the stick–slip motion [18]. Friction can also be reduced by appropriate chemical treatment of the contacting materials. For instance, friction on diamond-like carbon films can be lowered by two orders of magnitude after removal of sigma bonds. Molybdenum sulfide, a classical solid lubricant, has also been successfully tested as an extremely low-friction nanofilm. We might introduce the term *chemolubricity* to identify this form of superlubricity. We will not discuss these cases, and refer the reader to a recent volume edited by Erdemir and Martin [19].

2. Modeling single-contact friction on a crystal surface

The Tomlinson model is often used as a simple mechanistic approach to describe the friction in a single asperity contact as observed in a scanning force probe when the tip slides over an atomically flat surface. The general characteristics of the stick–slip motion manifested as a sawtooth-like modulation in the lateral force signal is well described by a model that has been formulated first by Prandtl [20] and then by Tomlinson [21]. In the simplest implementation, a point mass representing the tip is coupled by a spring to a constantly moving support, which is pulled along a sinusoidal surface potential with period a and amplitude E_0. Accordingly, for one dimension the total potential can be written as a sum of the periodic surface potential and the elastic energy which is stored in the spring

$$V = -\frac{E_0}{2}\cos\frac{2\pi x_{\mathrm{tip}}}{a} + \frac{1}{2}k(x_{\mathrm{tip}} - x)^2 \qquad (1)$$

where $x = vt$ is the position of the support (figure 1). The effective spring constant k of the pulling spring does not only represent the spring constant of the force sensor but also the respective compliance of tip and surface [22–24]. Several studies [16, 25, 18] revealed an effective stiffness in the order of 1 N m^{-1}, i.e. much smaller than the lateral stiffness of the cantilever. Hence, the lateral stiffness is dominated by the contact.

Obviously, this simple mechanical description can provide only qualitative interpretations of the underlying tribological processes; however, it accounts for the main physical features of atomic-scale friction such as the load dependence [16]. The temperature [26], velocity dependence [26, 27], and the distribution of jump forces [28] could be explained by additionally considering thermal activation. The model is in agreement with experiments studying the velocity dependence [26], the temperature dependence [29], and the jump force distribution [30]. However, the experimental situation is not well represented by one spring, since a one-spring model cannot reproduce both the resonance frequency of the cantilever and the lateral stiffness. Therefore, simulations have been extended to two-spring models where one spring represents the cantilever and the other spring the microscopic contact [31–35]. The Tomlinson model was also extended to the two-dimensional case, where tip jumps were observed in both x- and y-directions [36–39].

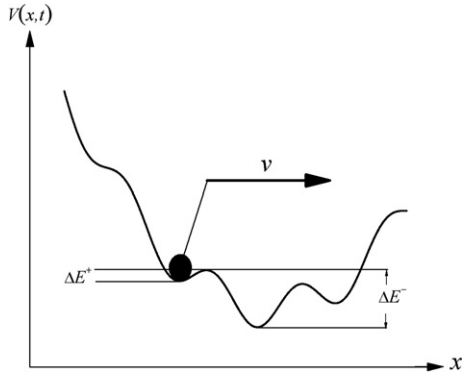

Figure 1. Schematic representation of a probing tip (black sphere) sliding across the time-dependent potential (1). The arrow represents the direction of motion, impressed by the driving cantilever. To reach the next equilibrium position the tip has to overcome an energy barrier ΔE^+. Once the tip jump has occurred, a reverse jump is hindered by a much higher energy barrier ΔE^-.

3. Static superlubricity

Considering a one-dimensional Tomlinson model, the lateral force on the tip in stable equilibrium conditions is obtained by differentiating equation (1) with respect to the position of the tip $\partial V/\partial x_{\mathrm{tip}} = 0$, thus

$$F = k(x - x_{\mathrm{tip}}) = \frac{\pi E_0}{a}\sin\frac{2\pi x_{\mathrm{tip}}}{a}. \qquad (2)$$

The relative strength of the surface corrugation E_0 with respect to the stiffness k is defined by the dimensionless parameter [16]

$$\eta = \frac{2\pi^2 E_0}{ka^2}.$$

Depending on the magnitude of η, several solutions are found for equation (2), which lead to metastable positions, and consequently to stick–slip instabilities and hysteresis effects while scanning. Therefore, the occurrence of dissipative stick–slip instabilities in the tip movement depends directly on the relation between the potential corrugation and the lateral stiffness. For values of $\eta < 1$ we have smooth sliding without energy dissipation, whereas for $\eta > 1$ stick–slip behavior is expected [16, 25]. Hence, for a hard spring and for a weakly corrugated potential the averaged friction force would become negligible. On the contrary, friction would occur for soft springs and for a highly corrugated potential. Since the corrugation becomes stronger with increasing applied load [16, 40], stick–slip occurs when the applied load exceeds a critical load for a given spring constant of a cantilever (figure 2(a)).

The transition from dissipative stick–slip to ultralow friction has been experimentally observed by Socoliuc *et al* [16] on NaCl in an ultrahigh vacuum (UHV) environment by a variation of the normal load applied to the contact. The observed lateral force traces showed excellent agreement with simulations based on the one-dimensional Prandtl–Tomlinson model. For small loads in the attractive force regime the stick–slip movement went over in smooth sliding without any

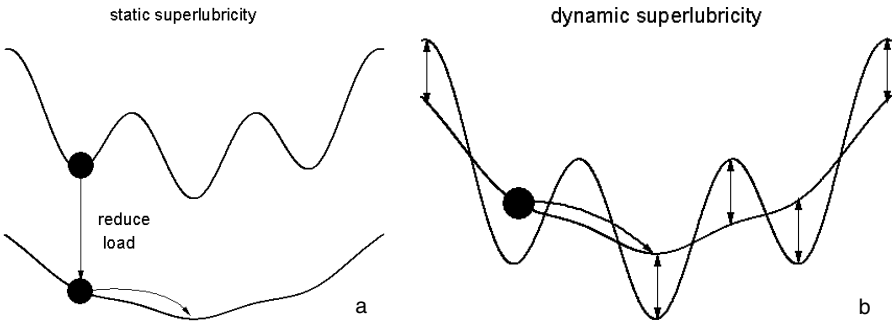

Figure 2. Schematic process of (a) static and (b) dynamic superlubricity. In case (a) the superlubric state is achieved by reducing the normal load (and consequently the tip–surface interaction) until the equilibrium of the tip becomes metastable and the tip gently moves across the surface lattice. In case (b) the tip–surface interaction oscillates at high frequencies, which results in superlubric motion even if the averaged normal load can be considerably higher.

abrupt jumps and hence dissipation decreases below a critical threshold. Recently, Medyanik *et al* confirmed these results on graphite by changing the load and lateral stiffness and showed also the transition to multiple slip regimes in an underdamped condition [25]. A similar transition from stick–slip to a low-friction state upon a variation of normal load has been observed by Takano and Fujihira on stearic acid crystals by FFM [41].

Recently, transitions from stick–slip to ultralow friction associated with a change of η were also observed within a unit cell of heteroepitaxial superstructures related to the small periodic rumpling induced at the interface between a heteroepitaxial film of KBr on NaCl(100) [42].

4. Dynamic superlubricity

In dynamic superlubricity, we assume that the corrugation of the tip–surface interaction periodically oscillates with time (figure 2(b)), i.e. a quantity $\alpha E_0 \cos \omega t$ is added to the constant E_0 in equation (1). The parameter α represents the relative strength of the periodic term in the energy corrugation compared to the constant term E_0, and takes values between 0 and 1. If the frequency ω is much larger than the 'washboard frequency' v/a, where v is the scan speed, the tip experiences the minimum corrugation value $E_0(1-\alpha)$ several times, and it can smoothly slide towards the next equilibrium position on the surface lattice without abrupt losses of stability. The condition for such dynamic superlubricity to be reached is

$$\alpha > 1 - \frac{1}{\eta}$$

as discussed in [17]. We notice that this dynamic superlubric regime can in principle be achieved for any value of the parameter η, provided that α is high enough.

Experimentally, dynamic superlubricity has been recently observed in UHV by applying an *ac* voltage to a silicon tip sliding on KBr and NaCl slabs approximately 1 mm thick, the back side of the samples being attached to a grounded electrode [17]. A strong variation of the tip–surface interaction was obtained if a resonance mode of the sliding system was excited, thus provoking strong vibrations of the tip perpendicular to the contact plane. Due to the presence of capacitive forces, this is also the case if the excitation is provided at half of these resonance frequencies. The decrease of the quality factor of the contact lever at higher harmonics leads to the maximum effect at the first resonance. Exciting a torsional resonance of the contacting lever did not result in superlubricity, contrary to what had been suggested by previous studies [40, 43].

These results could be extended to MEMS, where an *ac* voltage can be easily applied. In the case of atomic force microscopy, contact resonances can also be excited by the piezo-element routinely used to shake the cantilever in tapping and in non-contact mode. In such a case, sample materials are not limited to dielectrics, and dynamic superlubricity could be used as a powerful non-destructive imaging technique. Significant work in this direction is currently in progress within our group [44].

A reduction of friction caused by superimposed oscillations on the nanoscale has been also reported in different situations [45]. For instance, very low friction between oscillating junctions in the presence of an intercalated thin film has been measured by Heuberger *et al* [46] and Jeon *et al* [47] using surface force apparatus and AFM respectively. Gao *et al* reproduced this effect by molecular dynamics simulations, and related it to the relaxation of molecular flow [48]. Rozman *et al* suggested a method to control friction based on oscillations of the normal load aimed at suppressing chaotic stick–slip [49], whereas, in another theoretical work, Zaloj *et al* related the reduction of friction to increased separation (*dilatancy*) between the contacting surfaces [50]. Some experimental works also attribute a reduction of friction on the nanoscale to dilatancy effects [51, 52].

5. Other lubricity mechanisms

5.1. Thermolubricity

So far, we have not discussed thermal effects in nanoscale friction. Thermal vibrations can easily induce tip jumps. The warmer the (unlubricated) solid contact is, the more successful the activation process will be. As a result, less friction is expected, on average, at high temperature. The same conclusion holds if the sliding speed is reduced. In such a case, we can intuitively think that the slower the scan speed, the more

frequent jumping attempts will be. Experiments performed by our group on sodium chloride and copper surfaces in UHV revealed a logarithmic dependence of friction on the sliding velocity on three decades [26, 10]. This trend can be understood from the picture in figure 1. The tip jump towards the next equilibrium position along the scan direction is hindered by the energy barrier ΔE^+. This barrier decreases while the cantilever is pulling the tip, until the tip jumps as soon as ΔE^+ becomes of the order of $k_B T$, where T is the temperature of the contact. A simple analysis based on reaction rate theory leads to the logarithmic dependence of friction on the velocity. However, this result holds only in a well-defined range of velocities. If v exceeds a certain value (usually a few μm s^{-1} in FFM experiments) thermal activation becomes negligible [40] and various regimes are expected, depending on the damping mechanisms acting in the contact region [27, 28]. On the other hand, in the limit of slow scan velocities, backward jumps cannot be ignored. In such a case, Krylov *et al* demonstrated that friction should decrease linearly with v and become zero when $v \to 0$ [18]. Despite its elegance, *thermolubricity* is unfortunately of limited applicability in practice.

5.2. Structural lubricity

In the previous discussion we have also assumed that the FFM tip is atomically sharp. Even if the derivation remains substantially correct for contact areas formed by a few atoms, the situation changes when two wide surfaces slide one past the other. We limit our attention to the case of flat crystal surfaces with the same structure. In such a case, the reciprocal orientation of the crystal lattices becomes essential. If the two lattices are perfectly aligned, stick–slip is expected, as in the one-dimensional (1D) case. However, if the surfaces are misaligned, we can intuitively expect that, for every atom pulled in one direction, there is another atom pushed in the other direction, the two processes balancing and leading to zero friction when the surfaces are infinitely large [13].

After pioneer experiments by Hirano *et al* on mica [53] and Si(100) [54] the clearest evidence of this *structural lubricity* [55] was given by Dienwiebel and co-workers, who used a dedicated FFM with very close spring constants in fast and slow scan directions [56]. The experiment was performed on highly oriented pyrolytic graphite, at low humidity. As a result, the authors observed significant variations of friction with the orientation of the graphite surface. Frictional 'peaks' were observed at orientation angles of 0° and 60°, whereas friction became negligible far from these values. This result was attributed to structural lubricity, assuming that a graphite flake was removed from the surface and attached to the tungsten tip of their microscope in previous scanning. The fact that graphite flakes can indeed be detached and stick to a tungsten tip was recently supported by Merkle and Marks by TEM images [57]. Calculations of Verhoeven *et al* based on a modified Tomlinson model also discuss the contact between a rigid flake of finite size and a rigid crystal and show that the orientation dependence of friction provides information on the contact size and shape [58].

Structural lubricity can be easily suppressed by various mechanisms. In a recent experimental and theoretical study, Filippov *et al* showed that torque-induced reorientations of the sliding surfaces, coupled to the sliding motion, can lead to commensurability and high frictional forces [59]. The presence of mobile atoms between two surfaces can also result in finite friction, if the atoms tend to readjust in positions where they simultaneously match the geometry of both surfaces [60]. Elastic deformations of the bulk may cause geometric interlocking of the contacting surfaces, and cancel otherwise present structural lubricity [55]. Small changes in the surface roughness can also easily 'kill' the superlubric state [61].

6. Conclusions and outlook

In conclusion, the inapplicability of liquid lubricants at the nanoscale demands that we investigate solid friction between dry surfaces from an atomistic point of view. On dry nanocontacts, at least four mechanisms of friction reduction on the nanoscale have been recognized. Static lubricity is simply achieved by reducing the normal load below a well-defined threshold, depending on the surface potential and the elastic properties of the contacting materials. Dynamic lubricity exploits normal oscillations of the sliding objects and significantly increases the load threshold. The concept of thermolubricity implies that friction should vanish at infinitely slow relative speed due to thermal activation, whereas structural lubricity predicts negligible friction when two otherwise equal crystal surfaces slide past each other forming incommensurate contacts. Among these mechanisms, dynamic superlubricity seems to be the most suitable for applications to MEMS technology.

The investigation of superlubricity is strictly related to the development of atomic force microscopy. On the other hand, AFM can also benefit from these studies, as superlubricity might be used to image structures on the atomic scale in a non-destructive way. Extensions towards controlled manipulation of nanoparticles by AFM are also reasonable.

Acknowledgments

This work was supported by the Swiss National Science Foundation and the National Center of Competence in Research on Nanoscale Science.

References

[1] van Spengen W M 2003 *Microelectron. Reliab.* **43** 1049
[2] Kim S H, Asay D B and Dugger M T 2007 *Nano Today* **2** 22
[3] Williams J A and Le H R 2006 *J. Phys. D: Appl. Phys.* **39** R201
[4] Hu Y Z and Granick S 1998 *Tribol. Lett.* **5** 81
[5] Binnig G, Quate C F and Gerber Ch 1986 *Phys. Rev. Lett.* **56** 930
[6] Mate C M, McClelland G M, Erlandsson R and Chiang S 1987 *Phys. Rev. Lett.* **59** 1942
[7] Lüthi R, Meyer E, Haefke H, Howald L, Gutmannsbauer W, Guggisberg M, Bammerlin M and Güntherodt H J 1995 *Surf. Sci.* **338** 247

[8] Carpick R W, Dai Q, Ogletree D F and Salmeron M 1998 *Tribol. Lett.* **5** 91
[9] Ishikawa M, Okita S, Minami N and Miura K 2000 *Surf. Sci.* **445** 488
[10] Bennewitz R, Gyalog T, Guggisberg M, Bammerlin M, Meyer E and Güntherodt H J 1999 *Phys. Rev.* B **60** 11301
[11] Enachescu M, Carpick R W, Ogletree D F and Salmeron M 2004 *J. Appl. Phys.* **95** 7694
[12] Howald L, Lüthi R, Meyer E and Güntherodt H J 1995 *Phys. Rev.* B **51** 5484
[13] Hirano M and Shinjo K 1990 *Phys. Rev.* B **41** 11837
[14] Bruschi L, Fois G, Pontarollo A, Mistura G, Torre B, de Mongeot FB, Boragno C, Buzio R and Valbusa U 2006 *Phys. Rev. Lett.* **96** 216101
[15] Mason B L, Winder S M and Krim J 2001 *Tribol. Lett.* **10** 59
[16] Socoliuc A, Bennewitz R, Gnecco E and Meyer E 2004 *Phys. Rev. Lett.* **92** 134301
[17] Socoliuc A, Gnecco E, Maier S, Pfeiffer O, Baratoff A, Bennewitz R and Meyer E 2006 *Science* **313** 207
[18] Krylov S Y, Jinesh K B, Valk H, Dienwiebel M and Frenken J W M 2005 *Phys. Rev.* E **71** 065101
[19] Erdemir E and Martin J M 2007 *Superlubricity* (Amsterdam: Elsevier)
[20] Prandtl L 1928 *Z. Angew. Math. Mech.* **8** 85
[21] Tomlinson G A 1929 *Phil. Mag.* **7** 905
[22] Lantz M A, O'Shea S J, Hoole A C F and Welland M E 1997 *Appl. Phys. Lett.* **70** 970
[23] Lantz M A, O'Shea S J, Welland M E and Johnson K L 1997 *Phys. Rev.* B **55** 10776
[24] Carpick R W, Ogletree D F and Salmeron M 1997 *Appl. Phys. Lett.* **70** 1548
[25] Medyanik S N, Liu W K, Sung I H and Carpick R W 2006 *Phys. Rev. Lett.* **97** 136106
[26] Gnecco E, Bennewitz R, Gyalog T, Loppacher Ch, Bammerlin M, Meyer E and Güntherodt H J 2000 *Phys. Rev. Lett.* **84** 1172
[27] Reimann P and Evstigneev M 2004 *Phys. Rev. Lett.* **93** 230802
[28] Sang Y, Dube M and Grant M 2001 *Phys. Rev. Lett.* **87** 174301
[29] Sills S and Overney R M 2003 *Phys. Rev. Lett.* **91** 095501
[30] Schirmeisen A, Jansen L and Fuchs H 2005 *Phys. Rev.* B **71** 245403
[31] Reimann P and Evstigneev M 2005 *New J. Phys.* **7** 25
[32] Maier S, Sang Y, Filleter T, Grant M, Bennewitz R, Gnecco E and Meyer E 2005 *Phys. Rev.* B **72** 245418
[33] Krylov S Y, Dijksman J A, van Loo W A and Frenken J W M 2006 *Phys. Rev. Lett.* **97** 166103
[34] Abel D G, Krylov S Y and Frenken J W M 2007 *Phys. Rev. Lett.* **99** 166102
[35] Krylov S Y and Frenken J W M 2007 *New J. Phys.* **9** 398
[36] Fujisawa S, Kishi E, Sugawara Y and Morita S 1995 *Phys. Rev.* B **51** 7849
[37] Morita S, Fujisawa S and Sugawara Y 1996 *Surf. Sci. Rep.* **23** 1
[38] Fujisawa S, Yokoyama K, Sugawara Y and Morita S 1998 *Phys. Rev.* B **58** 49090
[39] Hölscher H, Schwarz U and Wiesendanger R 1996 *Europhys. Lett.* **36** 19
[40] Riedo E, Gnecco E, Bennewitz R, Meyer E and Brune H 2003 *Phys. Rev. Lett.* **91** 084502
[41] Takano H and Fujihira M 1996 *J. Vac. Sci. Technol.* B **14** 1272
[42] Maier S, Gnecco E, Baratoff A, Bennewitz R and Meyer E 2008 *Phys. Rev.* B submitted
[43] Tshiprut Z, Filippov A E and Urbakh M 2005 *Phys. Rev. Lett.* **95** 016101
[44] Gnecco E, Socoliuc A, Maier S, Gessler J, Glatzel Th, Baratoff A and Meyer E 2008 in preparation
[45] Urbakh M, Klafter J, Gourdon D and Israelachvili J 2004 *Nature* **430** 525
[46] Heuberger M, Drummond C and Israelachvili J 1998 *J. Phys. Chem.* B **102** 5038
[47] Jeon S, Thundat T and Braiman Y 2006 *Appl. Phys. Lett.* **88** 214102
[48] Gao J P, Luedtke W D and Landman U 1998 *J. Phys. Chem.* B **102** 5033
[49] Rozman M G, Urbakh M and Klafter J 1998 *Phys. Rev.* E **57** 7340
[50] Zaloj V, Urbakh M and Klafter J 1999 *Phys. Rev. Lett.* **82** 4823
[51] Dinelli F, Biswas S K, Briggs G A D and Kolosov O V 1997 *Appl. Phys. Lett.* **71** 1177
[52] Bureau L, Baumberger T and Caroli C 2000 *Phys. Rev.* E **62** 6810
[53] Hirano M, Shinjo K, Kaneko R and Murata Y 1991 *Phys. Rev. Lett.* **67** 2642
[54] Hirano M, Shinjo K, Kaneko R and Murata Y 1997 *Phys. Rev. Lett.* **78** 1448
[55] Müser M 2004 *Europhys. Lett.* **66** 97
[56] Dienwiebel M, Verhoeven G S, Pradeep N, Frenken J W M, Heimberg J A and Zandbergen H W 2004 *Phys. Rev. Lett.* **92** 126101
[57] Merkle A P and Marks L D 2007 *Appl. Phys. Lett.* **90** 064101
[58] Verhoeven G S, Dienwiebel M and Frenken J W M 2004 *Phys. Rev.* B **70** 165418
[59] Filippov A E, Dienwiebel N, Frenken J W M, Klafter J and Urbakh M 2008 *Phys. Rev. Lett.* **100** 046102
[60] Müser M H, Wenning L and Robbins M O 2001 *Phys. Rev. Lett.* **86** 1295
[61] Tartaglino U, Samoilov V N and Persson B N J 2006 *J. Phys.: Condens. Matter* **18** 4143